The influence of technique on the measured particle size distribution of complex nanoparticle systems

Å. K. Jämting, M. Roy, H. J. Catchpoole, M. Lawn, B. Babic, V. A. Coleman and J. Herrmann

National Measurement Institute Australia, Lindfield NSW 2070, Australia,

ABSTRACT

Characterization of the particle size distribution (PSD) of nanoscale systems presents numerous challenges, including detection and resolution limits of available instrumentation, statistical relevance (in single-particle methods), required prerequisite knowledge (for example, optical properties), and accounting for or overcoming matrix effects. All characterization instrumentation has inherent advantages, limitations and biases. To best understand what these are, a combination of different measurement techniques should be applied to measurements of a well-controlled system.

We present results from a comprehensive comparison of PSD measurements of four gold (Au) nanoparticle suspensions using six different characterization techniques: dynamic light scattering (DLS), particle tracking analysis (PTA), atomic force microscopy (AFM), transmission electron microscopy (TEM), differential centrifugation sedimentation (DCS), and asymmetric flow-field flow fractionation (AF4).

Keywords: nanoparticle characterization, measurement techniques, comparison

1 INTRODUCTION

Accurate and reliable characterization of nanoparticles is crucial for both industrial applications and studies of their toxicological and environmental impacts. Particle size distribution (PSD) has been widely recognised as one of the key parameters that should be reported in studies of nanoscale systems [1], [2] since particle size can be related to, amongst other things, product functionality, toxicological response and transport, and clearance and/or persistence pathways in environmental and mammalian systems [3].

2 EXPERIMENTAL DETAILS

The four samples analyzed in this study comprised aqueous suspensions of citrate stabilized Au colloids (BBInternational, UK); two with mono-modal PSDs (nominal mean diameters (TEM): NPS 1: 20 nm and NPS 2: 100 nm), and two with bi-modal PSDs (NPS 3 and NPS 4). NPS 3 and NPS 4 were produced by mixing volumina of NPS 1 and NPS 2 in ratios to generate equal peak heights in intensity-weighted light scattering PSD measurements (NPS 3) and in number-weighted PSD measurements (NPS 4), respectively.

Six characterization techniques were used for this study. Dynamic light scattering (DLS) measurements in batch mode were carried out using a Malven Zetasizer Nano ZS (Malvern Instruments, Malvern, UK). The respective Au suspensions were diluted 1:4 with a 2 mmol sodium chloride (NaCl) suspension. Vortex mixing was performed to ensure sample homogeneity. All DLS measurements were carried out on temperature equilibrated samples at an instrument temperature of 20 °C.

Particle tracking analysis (PTA) was carried out on samples diluted with 2 mmol NaCl using a Nanosight LM10 (NanoSight Ltd., Amesbury, UK) with a 628 nm laser source and a high sensitivity camera (Hamamatsu C11440 Orca-flash 2.8, Hamamatsu Photonics K.K., Hamamatsu City, Japan). The measurement temperature was 22–23 °C. The generated videos were analysed using the Nanosight software, v. 2.3.

Atomic force microscopy (AFM) results were generated using an Asylum Research MFP-3D SA (Asylum Research, Santa Barbara, USA) operating in intermittent contact mode. AFM samples were prepared by first functionalising mica substrates with 0.1 % poly-l-lysine before drop casting the Au suspension onto the substrate. The particle height was determined using the "Particle & Pore Analysis" function in SPIP software (Image Metrology A/S, Hørsholm, Denmark).

For transmission electron microscopy (TEM) analysis, the Au suspensions were diluted with ultrapure water (18 MΩ cm; MilliQ, Millipore, USA) and then drop cast onto 300 mesh copper grids with an ultra-thin carbon layer. The TEM micrographs were obtained using a JEOL 2100 TEM (JEOL Ltd, Tokyo, Japan) operating at 200 kV, equipped with a Gatan Ultrascan 1000 camera (1024×1024 pixels). All images were analysed using ImageJ software v. 1.45s [4], and the equivalent spherical diameters were derived from the measured areas of the particles.

Differential centrifugal sedimentation (DCS) measurements were performed on a CPS disc centrifuge model 24000UHR (CPS Instruments, Stuart, FL, USA) operating at 24 000 rpm in an 8–24 % sucrose density gradient. A 60 nm gold reference material (RM 8013), from the National Institute of Standards and Technology (NIST) (NIST, Gaithersburg, MD, USA), with an assumed density of 19.3 g cm^{-3} was used for calibration.

For the asymmetric flow-field flow fractionation (AF4) experiments, a Wyatt Eclipse 3+ system (Wyatt Technology, Santa Barbara, CA, USA) with channel length 26.55 cm (tip to tip) and channel thickness of 0.035 cm, coupled with an Agilent 1200 HPLC system (Agilent Technologies, Santa Clara, CA, USA) was utilized. A regenerated cellulose membrane (Millipore PLGC, Wyatt

Technology) with a molecular weight cut-off of 10 kDa was used as the channel wall. The detection system is equipped with an 18 angle light scattering detector (DAWN HELEOS 2, Wyatt Technology), a DLS detector (DynaPro, Wyatt Technology) and a UV-vis diode array detector (DAD1200, Agilent Technologies) with a spectral range from 190 nm to 900 nm.

3 RESULTS AND DISCUSSION

All the techniques used in this study provided reproducible measurement results for the PSD of NPS 1 and NPS 2, detecting a single population of particles with diameters close to the nominal mean values. The mean results for these two samples when measured with the six different measurements techniques are shown in Table 1.

Table 1. Mean particle diameters measured using six different techniques for samples NPS 1 and NPS 2.

	NPS 1 (nm)	Standard deviation (nm)	NPS 2 (nm)	Standard deviation (nm)
DLS-batch	21.5	0.2	96.6	0.1
PTA	22.2 (mode)	1.5	87.3 (mode)	5.8
AFM	16.5	0.1	86.8	0.6
TEM	19.0	0.3	108.6	8.2
DCS	17.2	0.2	103.5	0.9
AF4-DLS	21.1	1.6	93.5	0.6

For the more complex samples, differences in the measured PSDs were more pronounced, reflecting the differences between each measurement technique's ability to distinguish the two populations, as illustrated in Figure 1.

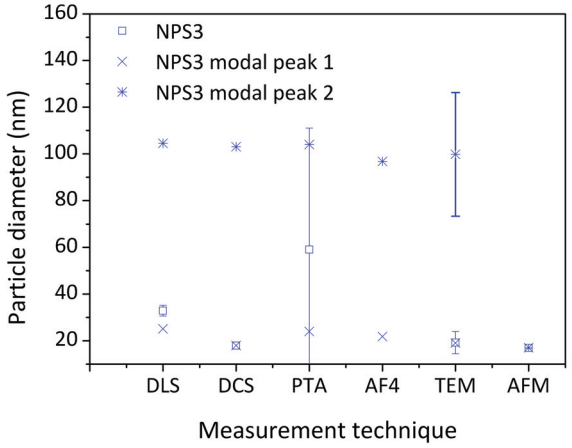

a)

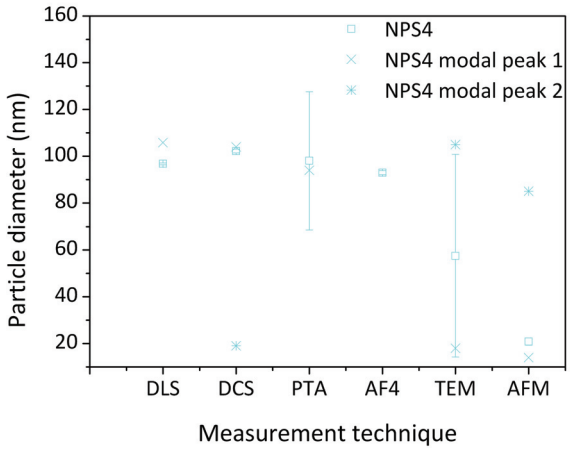

b)

Figure 1. Combined data from the measurements of NPS 3 (a) and NPS 4 (b). The graphs show the mean diameter of the PSD generated by each technique, and the modal values for the two particle populations (where detected).

Using DLS in batch mode, it was possible to clearly differentiate between the two peaks in the NPS 3 sample, where the number of small particles in the suspension is significantly greater than the larger particles (Figure 2). The NPS 4 sample, however, proved very challenging for DLS, with the average measured size indicating that the signal from the larger particle population completely overwhelmed the signal from the smaller particles.

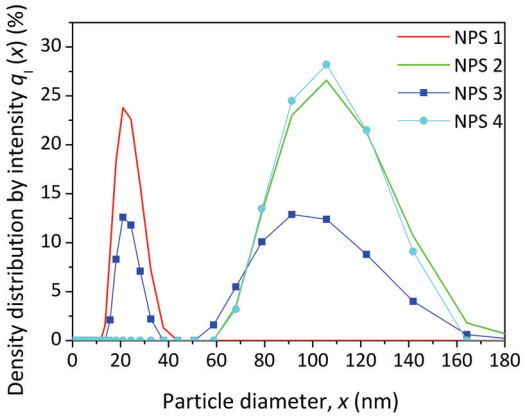

Figure 2. Intensity-weighted PSDs of the four nanoparticle suspensions, measured using DLS.

The PTA technique tracks the Brownian motion of individual particles and hence provides a number based measurement of the hydrodynamic diameter. The instrument's detection limit is determined by the scattering properties of the particles and the camera resolution and frame rate. The modal values presented here for samples NPS 1 and NPS 2 agree well with the nominal values, as well as with the measurements from the other techniques (see Figure 3). The more complex samples proved to be a

greater challenge. The smaller particle population scatters much less light and is thus harder to detect, so the camera settings have to be optimised for this population. The larger particles scatter light much more intensely, and halo-like diffraction rings are formed around them. This results in noisy videos which are challenging to analyze. For very dilute suspensions, it was possible to detect the two populations, but the number of detected particles in the larger population was much greater than expected from the sample design. The population of larger particles in NPS 4 dominated the images, and the camera was barely able to detect the scattering signal from the smaller particles. Attempts were made to use a camera with lower resolution where the video can be separated into two with independent shutter and gain, but this did not improve the detection ability significantly.

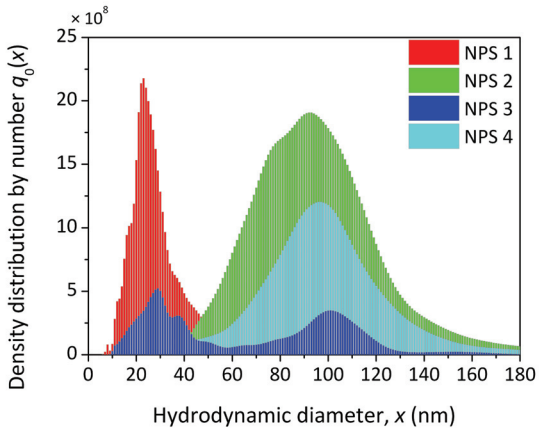

Figure 3. Number-weighted PSDs for the four nanoparticle suspensions, measured using PTA.

In contrast, the microscopy-based methods such as AFM and TEM are more suited to resolving the true PSD in NPS 4, but struggled to detect the comparatively few larger particles in the NPS 3 sample as illustrated in the TEM micrograph in Figure 4.

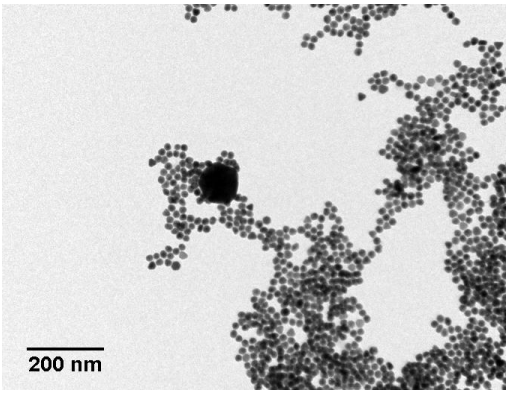

Figure 4. TEM image of NPS 3, illustrating the particle sub-populations with concentrations adjusted to produce equal peak heights in the intensity-weighted PSD in DLS measurements.

The population of larger particles in NPS 3 was not detected by AFM, even though multiple sample regions were imaged. The measured size of the smaller particles in NPS 3 agreed very well with the measurements of the NPS 1 sample. The analysis of the TEM images of NPS 4 indicated a number ratio of small to large particles of 1:1.6, which was close to the original sample design. This was not the case for the AFM measurements, where a much greater number of small particles were detected compared to the larger particles (8.7:1). This observation illustrates how a limited field of view can limit a microscopy technique's ability to obtain a representative overview of the entire sample and hence generate images that are truly representative of the entire population. The modal diameter of the larger particles measured by AFM in NPS 4 agrees well with the measurements of NPS 2, whereas the modal diameter of the smaller particles is 2.5 nm smaller than the measured mean diameter in NPS 1. The cause of this discrepancy may be due to scan size and resolution.

The DCS method, where the particles are separated according to their Stokes diameter using centrifugal force, was able to resolve the PSD for all samples. NPS 4 (Figure 5) gave very distinct signal for both the particle populations whereas the signal from the larger particle population in NPS 3 was only barely detectable .

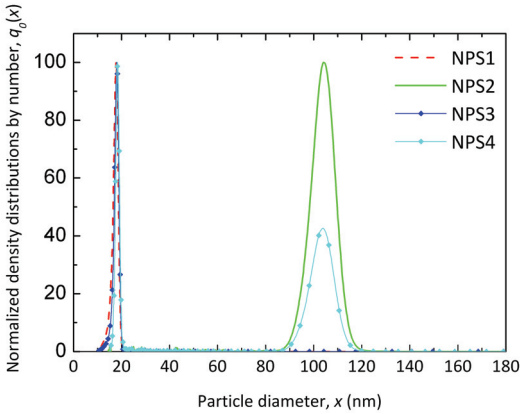

Figure 5. Normalized number-weighted PSDs, measured using DCS, for the four nanoparticle suspensions.

For the other separation-based method, AF4, detection of the different particle populations proved more difficult. This technique separates particles based on their hydrodynamic diameter, using a fluid cross-flow to achieve the separation. Both the light scattering detector and the UV-vis detector successfully detected the particles in NPS 1 and NPS 2. The mean diameter results shown in Table 1 were obtained with the DLS detector. For NPS 3, the population of smaller particles was also clearly detected as shown in Figure 6. The larger particles in this sample were more difficult to detect and required substantial method development prior to successful detection. The two particle populations in NPS 4 were detected only by the UV-vis detector since the signal from the population of smaller particles was not strong enough for the DLS detector, and

the larger particles scatter light too strongly for the DLS detector to make meaningful measurements.

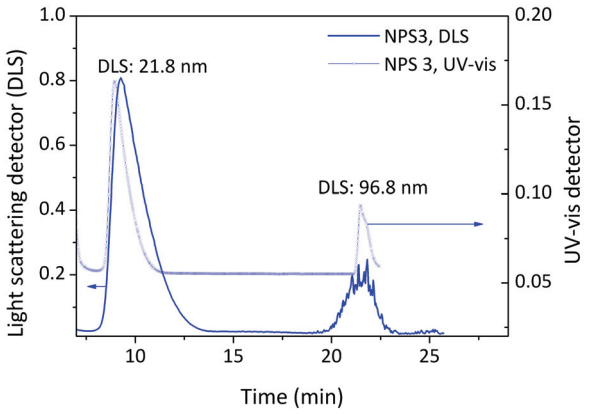

Figure 6. Elution fractogram from the AF4 measurement of NPS 3, showing the signals from the DLS detector and the UV-vis detector.

4 SUMMARY AND CONCLUSIONS

The results of this study clearly demonstrate the strengths and weaknesses of the different measurement techniques used to characterize suspensions with both mono-modal and bi-modal PSDs. All the techniques used provided measurement results of the mean particle diameters for the mono-modal samples (NPS 1 and NPS 2) which were consistent with the nominal values provided by the particle manufacturer.

For the more complex samples (NPS 3 and NPS 4), the results clearly highlight the inherent biases of different measurement techniques. The intensity-dependent signal from the DLS was strongly affected by the population of larger particles, and the results for NPS 3 and NPS 4 do not provide a true representation of the samples. The single-particle PTA technique is also limited by the scattering properties of these bi-modal samples. It was possible to detect the two populations in NPS 3, but the smaller population in NPS 4 was not detected. The results from the microscopy-based techniques (TEM and AFM) show that great care had to be taken to generate results that were truly representative of the sample composition. In the case of AFM, none of the larger particles were detected in NPS 3 despite acquiring images of multiple areas of the sample. For the techniques where separation of the suspension prior to measurement occurs, the two populations of particle sizes present in the samples could be determined by careful examination of the results. The results from the AF4 measurements of NPS 4 suggest that the use of more than one detector can be useful to facilitate more thorough characterization.

These findings are an important tool for scientists who perform and interpret size measurements on nanoscale particle systems, as they help to understand the advantages, limitations and biases of the different types of instrumentation.

Certain trade names and company products are mentioned in the text in order to adequately specify the experimental procedure and equipment used. In no case does such identification imply recommendation or endorsement by the National Measurement Institute Australia, nor does it imply that the products are necessarily the best available for the purpose.

REFERENCES

[1] G. Oberdorster, A. Maynard, K. Donaldson, V. Castranova, J. Fitzpatrick, K. Ausman, *et al.*, "Principles for characterizing the potential human health effects from exposure to nanomaterials: elements of a screening strategy," Particle and Fibre Toxicology, vol. 2, p. 8, 2005.

[2] T. P. J. Linsinger, G. Roebben, D. Gilliland, L. Calzolai, F. Rossi, N. Gibson, *et al.*, "Requirements on measurements for the implementation of the European Commission definition of the term 'nanomaterial'," European Commission, Joint Research Centre, Luxembourg, 2012.

[3] I. Montes-Burgos, D. Walczyk, P. Hole, J. Smith, I. Lynch, and K. Dawson, "Characterisation of nanoparticle size and state prior to nanotoxicological studies," Journal of Nanoparticle Research, vol. 12, pp. 47-53, 2010.

[4] *ImageJ*. Available at: http://rsbweb.nih.gov/ij/